Prediction of Thermal Deformation for a Ball Screw System Under Composite Operating Conditions

A. S. Yang, S. Z. Chai, H. H. Hsu, T. C. Kuo, W. T. Wu, W. H. Hsieh and Y. C. Hwang

Abstract The position error of a feed drive system is mostly caused by thermal deformation of a ball screw shaft. A high-speed ball screw system can generate massive heat with greater thermal expansion produced, and consequently have a negative effect on the positioning accuracy. In this study, we applied the computational approach using the finite element method (FEM) to simulate the thermal expansion process for estimating the deformation of the ball screw system. In the numerical analysis, the deformation of the ball screw shaft and nut was modeled via a linear elasticity approach along with the assumption that the material was elastic, homogeneous, and isotropic. To emulate the reciprocating movements of the nut at the speeds of 20, 40 and 60 m/min corresponding to the screw shaft, we also employed a three-dimensional unsteady heat conduction equation with the heat generation from the main sources including the ball screw shaft, nut and bearings as the heat transfer model to solve the temperature distributions for determining the temperature rises and axial thermal deformations in a ball screw

A. S. Yang · S. Z. Chai · H. H. Hsu
Department of Energy and Refrigerating Air-Conditioning Engineering, National Taipei University of Technology, Taipei 106, Taiwan
e-mail: asyang@ntut.edu.tw

T. C. Kuo · W. H. Hsieh (✉)
Department of Mechanical Engineering, and Advanced Institute of Manufacturing with High-tech Innovations, National Chung-Cheng University, Chiayi 621, Taiwan
e-mail: imewhh@ccu.edu.tw

W. T. Wu
Department of Biomechatronics Engineering Nation Pingtung University of Science and Technology, Pingtung 912, Taiwan
e-mail: azbennywu@gmail.com

Y. C. Hwang
HIWIN Technologies Corp, Taichung 408, Taiwan
e-mail: lawrence@mail.hiwin.com.tw

shaft under composite operating conditions. The simulated results demonstrated that the countermeasures must be taken to thermally compensate great deterioration of the positioning accuracy due to vast heat production at high rotating speeds of shaft for a ball screw system.

Keywords Ball screws · FEM · Heat transfer model · Machine tool · Positioning accuracy · Thermal deformation

1 Introduction

The performance of a ball screw feed drive system in terms of speed, positioning accuracy and machine efficiency plays a very important role in product quality and yield in manufacturing industries primarily including machine tools, semi-conductors, optoelectronics, and so on. Considering a high-speed precision ball screw system, the occurrence of contact surfaces (such as the interfaces between the ball and nut grooves, the ball and screw grooves, and the bearing and shaft) produces contact friction at these junctions. The friction of the nut and ball bearings entails a sudden and violent heating of balls, and in turn results in the temperature rises of the ball screw, leading to mechanical micro- deformations and an overheating of the coolant. Such a temperature heating of ball screw could also cause significant thermal deformations deteriorating the ball screw system accuracy in mechatronics tools or instruments [1].

The development of fabrication technology for a variety of applications necessitates high-precision apparatuses for achieving remarkably delicate goods with high output [2]. As indicated by Bryan [3], the thermal induced error in precision parts has still been the key setback in the industry. Substantial efforts were done on the machine tools, thermal behavior and thermal error compensation on the spindles, bearings and ball screws, respectively. Ramesh et al. [4] and Chen [5] carried out the air-cutting experiments to reproduce the loads under actual-cutting situations. To adjust the thermal conditions of the machine tool, Li et al. [6] conducted the tests of varying spindle speed for controlling the loads. The performance of a twin-spindle rotary center was experimentally evaluated by Lo et al. [7] for particular operating settings. Afterward, Xu et al. [8] incorporated the contact resistance effect into a thermal model for simulation of machine tool bearings. Koda et al. [9] produced an automatic ball screw thermal error compensation system for enhancement of position accuracy.

The frictional process from a high-speed ball screw system essentially released tremendous amounts of heat and results in the continuing temperature increase and thermal expansion, leading to deterioration of the positioning accuracy. In this investigation, we considered the heat generation from two bearings and the nut as the thermal loads with the prescribed heat flux values imposed on the inner surfaces of grooves between the bearings and nut of the ball screw system.

The convection boundary conditions were also treated for solid surfaces exposed to the ambient air. A FEM-based thermal model was developed to resolve the temperature rise distribution and in turn to predict the thermal deformation of the ball screw. In addition, simulations were conducted to appraise the influence of composite operating conditions in terms of different speeds (1,000, 2,000 and 3,000 rpm) as well as moving spans (500 and 900 mm) of the nut on the temperature increases and thermal deformations of a ball screw shaft.

2 Description of Ball Screw System

Figure 1 presents a schematic diagram of a ball screw feed drive system, encompassing a ball screw and driving unit. A continuous advance and return movement of the ball screw takes place in the range of 900 mm. It has 20-mm lead, 41.4-mm ball center diameter (BCD) and 1,715-mm total length. The outer and inner diameters of the screw shaft are 40 and 12.7 mm, respectively. Table 1 presents the parameters of main components for the ball screw drive system, which really contains the ball screw shaft, ball screw nut and bearings.

Figure 2 illustrates the moving velocity of the screw nut. This investigation considers the reciprocating movements of the nut at a maximum speed of 40 m/min pertaining to the screw shaft with a time period of 3.43 s and acceleration/deceleration of ± 2.1 m/s^2 as the baseline study case.

3 Computational Analysis

The physical model in this study investigates the thermal expansion process in a ball screw system. Essentially, heat is generated mainly from the friction between the ball and nut grooves as well as the ball and screw grooves. In view of the fact that a string of balls filled the grooves between the screw and nut are rotating very fast, the heat has been distributed evenly over the inner surface of raceways. The nut and two bearings are modeled as the fixed thermal loads imposed on the ball screw shaft. The thermal resistance resulting from the lubrication oil film between the balls and raceways is assumed to be ignored here attributable to a very thin layer of oil film, and the effect of heat conduction by means of the lubricant and thermal deterioration is negligible. Numerical calculations were performed by the FEM software ANSYS$^®$ to investigate the thermal behavior of a ball screw [10]. The theoretical formulation was based upon the time-dependent three-dimensional heat conduction equation for a ball screw system. The governing equations are stated as follows:

$$k\left(\frac{\partial^2 T}{\partial x^2} + \frac{\partial^2 T}{\partial y^2} + \frac{\partial^2 T}{\partial z^2}\right) = \rho c \frac{\partial T}{\partial t}. \tag{1}$$
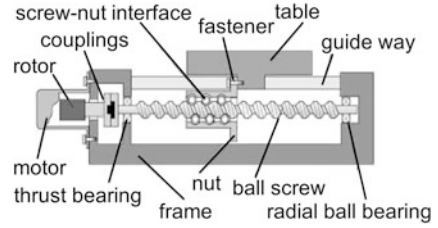
Fig. 1 Schematic of a ball screw feed drive system

Table 1 Main component parameters of the ball screw feed drive system

Ball screw shaft		Ball screw nut	
Total Length (mm)	1,715	Type	FDC
Thread Length (mm)	1,295	Length (mm)	143.4
LEAD (mm)	20	Diameter (mm)	70
BCD (mm)	41.4		
Outer diameter(mm)	40		
Inner diameter (mm)	12.7	*Bearing*	
Line number	2	Type	TAC
Contact type	4 points	OD (mm)	30
Ball diameter (mm)	6.35	ID (mm)	12.7

Fig. 2 Moving velocity of the screw nut with respect to the screw shaft
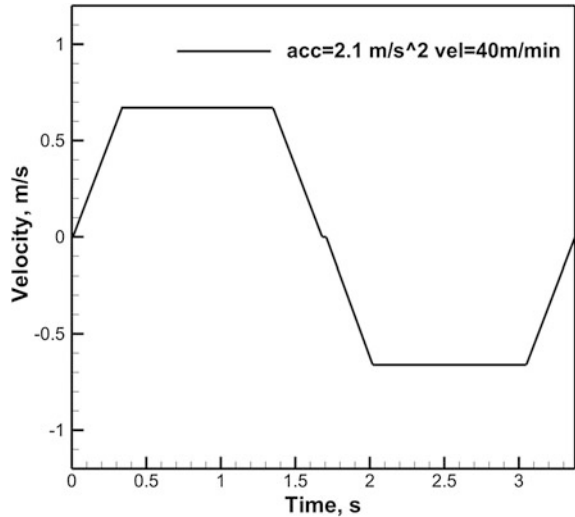
The symbols ρ, c, k and T mean the density, specific heat, thermal conductivity, and temperature of the ball screw shaft and nut, respectively. Here the temperature T is a function of the spatial coordinates (x, y, z) and time. The ρ, c, k values for computations are 7,750 kg/m^3, 480 J/kg-°C and 15.1 W/m-°C. Figure 3 exhibits the heat generation by the nut and bearing for a period of 3.43 s. The friction effect
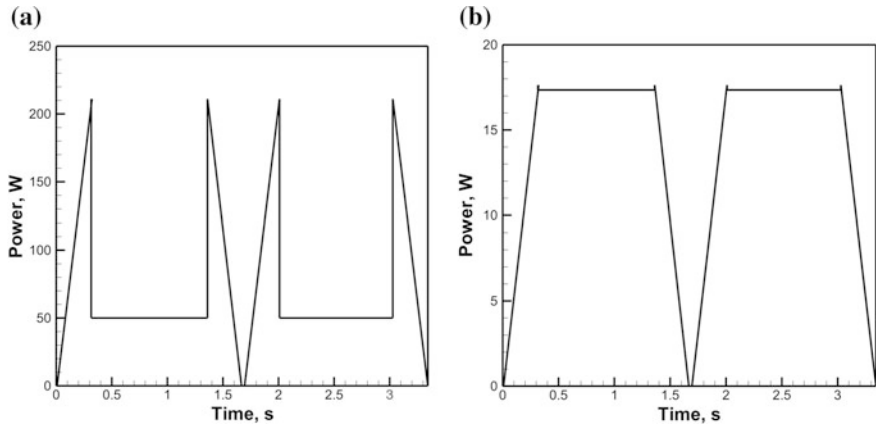
(a)

(b)

Fig. 3 Heat generation by **a** nut and **b** bearing for a period of 3.43 s

between the balls and raceways of the nut and bearings is the most important cause for temperature increase.

Given that the load of the nut contains two parts: the preload and dynamic load, $\dot{G}_{nut}$, the heat generation by the nut (in W), can be described as [11, 12]:

$$\dot{G}_{nut} = 0.12\pi f_0 v_0 nM. \tag{2}$$

Here f_0 is a factor determined by the nut type and lubrication method; v_0 is the kinematic viscosity of the lubricant (in m^2/s); n is the screw rotating speed (in rpm); M is the total frictional torque of the nut (in N-mm). In this research, $\dot{G}_{bearing}$ is the heat generated by a bearing (in W), defined as below [13].

$$\dot{G}_{bearing} = 1.047 \times 10^{-4} nM. \tag{3}$$

The variables n is the rotating speed of a bearing and M is the total frictional torque of bearings, including the frictional torque due to the applied load and the frictional torque due to lubricant viscosity.

The convective heat transfer coefficient h (in W/m^2-°C) is computed [14] by

$$h = Nuk_{fluid}/d. \tag{4}$$

Here Nusselt number $Nu = 0.133Re^{2/3}Pr^{1/3}$, while the variables Re and Pr represent Reynolds number and the Prandtl number. The sign k_{fluid} is the thermal conductivity of the surrounding air and d is the outer or inner diameter of the screw shaft (mm). More detailed information can be found in Ref. [15].

In this study, the ball screw is modeled using a linear elasticity approach and assumed as the elastic, homogeneous, and isotropic material. The governing equations for the ball screw deformation are as follows:

$$\rho \frac{\partial^2 v_x}{\partial t^2} = \frac{\partial \sigma_x}{\partial x} + \frac{\partial \tau_{yx}}{\partial y} + \frac{\partial \tau_{zx}}{\partial z} + \rho g_x. \tag{5}$$

$$\rho \frac{\partial^2 v_y}{\partial t^2} = \frac{\partial \sigma_y}{\partial y} + \frac{\partial \tau_{xy}}{\partial x} + \frac{\partial \tau_{zy}}{\partial z} + \rho g_y. \tag{6}$$

$$\rho \frac{\partial^2 v_z}{\partial t^2} = \frac{\partial \sigma_z}{\partial z} + \frac{\partial \tau_{xz}}{\partial x} + \frac{\partial \tau_{yz}}{\partial y} + \rho g_z. \tag{7}$$

The variables $\vec{v}$, $\vec{\sigma}$ and $\vec{\varepsilon}$ symbolize the displacement, stress and strain vectors (tensors).

$$\vec{\sigma} = D(\vec{\varepsilon} - \varepsilon^{th}) \tag{8}$$

The symbol ε^{th} is the thermal strain. Given the assumption of a linear elastic response, the stress-strain relationship is given by $\vec{\sigma} = D\vec{\varepsilon}$, where D has the form

$$D = \begin{pmatrix} \lambda + 2G & \lambda & \lambda & 0 & 0 & 0 \\ \lambda & \lambda + 2G & \lambda & 0 & 0 & 0 \\ \lambda & \lambda & \lambda + 2G & 0 & 0 & 0 \\ 0 & 0 & 0 & G & 0 & 0 \\ 0 & 0 & 0 & 0 & G & 0 \\ 0 & 0 & 0 & 0 & 0 & G \end{pmatrix} \tag{9}$$

$$\lambda = \frac{vE}{(1 + v)(1 - 2v)}, \quad G = \frac{E}{2(1 + v)} \tag{10}$$

$$\varepsilon^{th} = \Delta T (\alpha, \quad \alpha, \quad \alpha, \quad 0, \quad 0, \quad 0,)^T \tag{11}$$

D is the elasticity matrix consisting of the material properties, whereas the properties of E, v and α are the Young's modulus, the Poisson's ratio and the coefficient of thermal expansion (CTE). In this investigation, the values of Young's modulus, Poisson's ratio and CTE of the ball screw are set to be 1.93×10^{11} Pa, 0.31 and 1.16×10^{-5} m/m-°C. The term $\Delta T = T - T_{ref}$, T_{ref} is the initial temperature of 27 °C. A finite element method was used to solve the ball screw model in accordance with the principal of virtual work. For each element, displacements were defined at the nodes and the associated displacements within the elements were subsequently obtained by means of interpolation of the nodal values by the shape functions. The strain-displacement and stress-strain equations for structure were solved with the Gaussian elimination method for sparse matrices [10].

4 Experimental Measurements

Experimental measurements were conducted to determine the time-dependent distributions of temperature, temperature rise and thermal deformation for validation of the thermal model by FEM and evaluate the performance of the cooling system. Figure 4 illustrates a schematic diagram of the experimental set up, containing the ball screw, driving unit, LNC controller, thermal/laser detection system for measuring temperature/deformation and linked data acquisition system. A continual forward and backward movement of ball screw ensued in a 900-mm range, having 20 mm lead, 41.4 mm BCD and 1,715 mm total length. The data processing module consisted of four thermal couples as well as a high-precision Renishaw XL-80 laser system with the test data recorded for every 600 s.

5 Results and Discussion

Simulations were attained by the FEM software ANSYS® to predict the thermal and deformation characteristics of a ball screw. In the analysis, we modeled a string of balls as a coil-like circular band fully filled the interior surface of raceways between the screw and nut. Figure 5 displays the numerical grids for system simulations. The mesh setup had three unstructured sections, such as the bearings, shaft and coil-like circular band. Finer grids were paced in the areas near the grooves and the solid surfaces. The average cell length was approximately 0.0015 m with the least spacing of 0.0006 m to resolve the steep variations of thermal properties near heat sources. The predictions of transient temperature distributions on the surface of the ball screw with different grids and time steps suggested that grid independence could be attained using a mesh setup of 1,367,867 grids with a time step of 5 s.

In simulations, the reciprocating movements of the nut was at a speed of 40 m/min respecting to the screw shaft with a 3.43-s period. The analysis was based on the rotational speed of 3,000 rpm and the initial temperature of 27 °C. During the continual operations, Fig. 6 illustrates the temperature and thermal deformation distributions along the axial distance of hollow ball screw shafts at t = 3,600 s. The frictional heat produces the temperature rise with high temperatures occurred in the core areas of the ball screws for hollow ball screws.

In the structure analysis, the left side of the ball screw was treated as the free end with the right side maintained as the fixed-end condition. The thermal loads from the temperature distribution predictions were then input to solve the thermal deformation. The predicted results indicated relatively larger local thermal deformations near the high temperature regions occurred at the center of the shaft in general. The thermal deformation distributions showed a great reduction in thermal expansion for the hollow shaft at the left end of the screw.
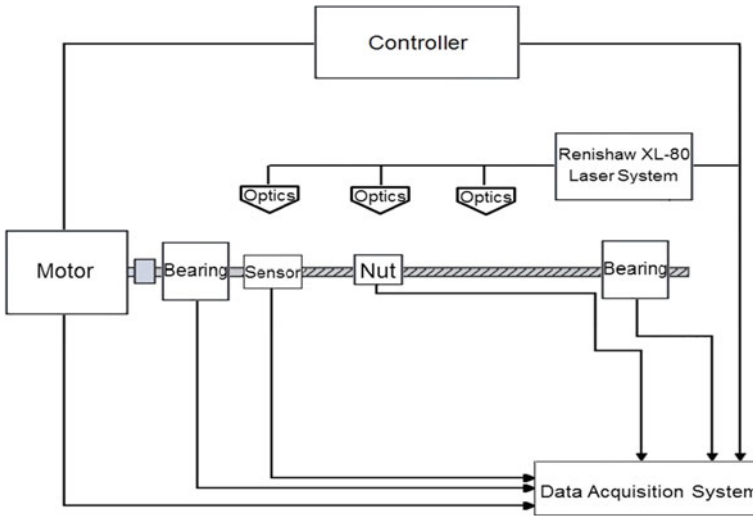
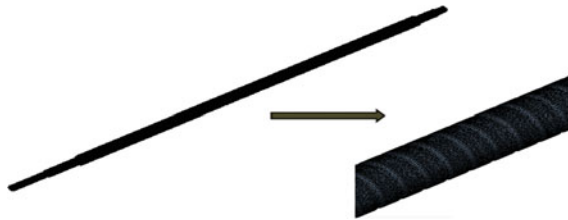**Fig. 4** Schematic diagram of the experimental set up

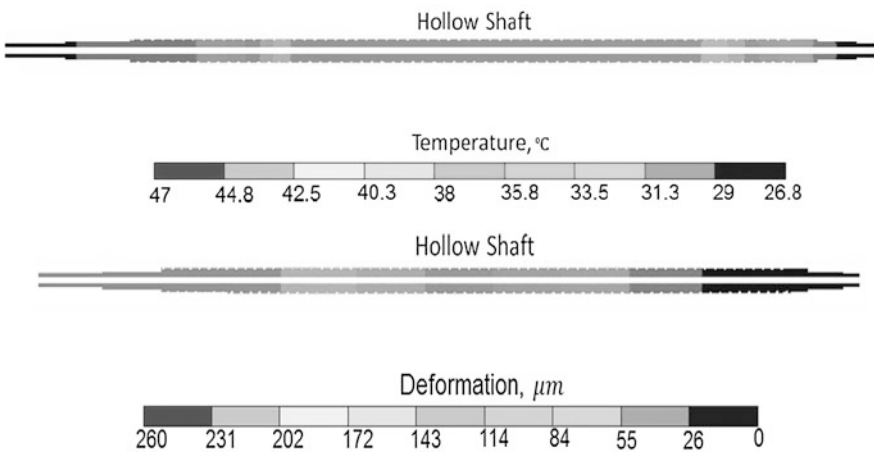**Fig. 5** Numerical grids of ball screw shaft

Fig. 6 Temperature and thermal deformation distribution of ball screw shafts at t = 3,600 s

Fig. 7 Comparison of
prediction with measured
temperature rise data along
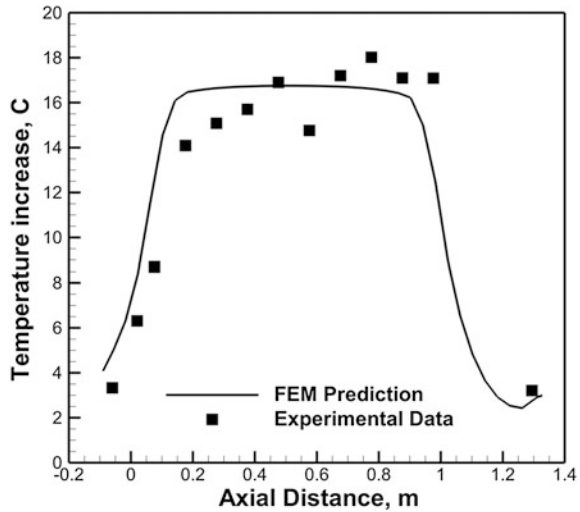the axial distance of ball
screw at t = 3,600 s

Figure 7 illustrates a comparison of the prediction with the measured temperature rise data along the axial axis of hollow ball screw at t = 3,600 s. The calculated temperature rise distribution was compared with the measurements of different positions. Overall, the results clearly indicated that the FEM model relatively over-predicted the temperature increase (i.e. 17.7 °C in the central area of the shaft) with the discrepancy within approximately 18.7 % in the axial distance of 0.15 to 0.4 m, showing that the simulation software may reasonably simulate the thermal expansion phenomenon.

As far as the transient developments of temperature rises are concerned, Fig. 8 illustrates a comparison of time history of the predictions with measured temperature rises at three locations for the hollow ball screw. At the pre-specified axial distances of 0.05, 0.68 and 1.62 m, all three temperature rise profiles grew quickly in the early stage and tended to level off toward their steady-state values of 2.73, 17.2 and 2.66 °C for the test points of 1, 2 and 3, respectively, at t = 3,600 s. Due to massive heat generated in continuing operations, both the predicted measured results of the test point 2 show a higher temperature rise with the difference under 1.93 %, revealing the accuracy of the FEM simulations.

In order to verify the thermal and structural models by FEM, Fig. 9 illustrates a comparison of the prediction with measured thermal deformation data along the axial distance of hollow ball screw at t = 3,600 s. The thermal deformation along the axial direction was measured using a laser interferometer, for comparison with the calculated results. It can be clearly seen that the deformations from the FEM predictions and the experimental results were fairly close, deviating below 9.1 % for the axial distance from 0.2 to 0.9 m. Nevertheless, as compared to the test data, the over-predicted deformation was noted with a large error appeared at the axial distance of 0.1 m owing to the over-estimation of temperature rise in this associated area.

Fig. 8 Comparison of the
time history of the predictions
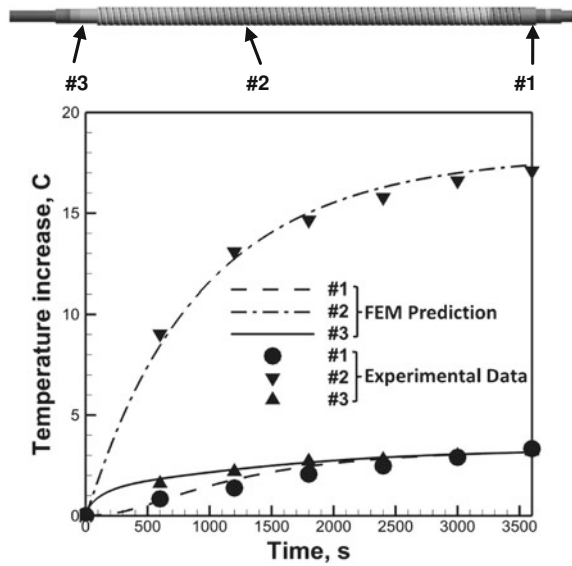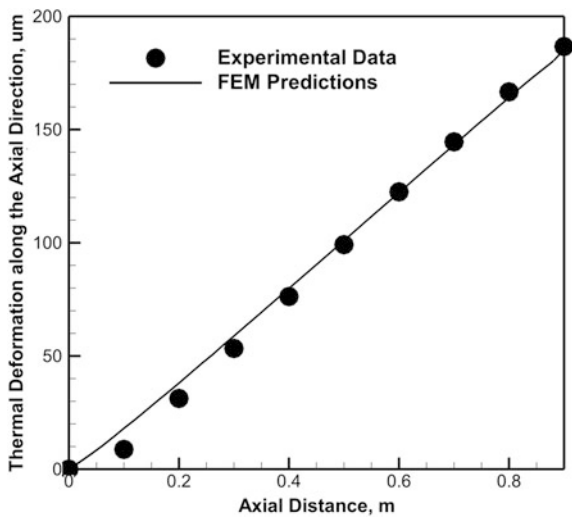with measured temperature
rises at three locations for ball
screw

Fig. 9 Comparison of the
prediction with measured
thermal deformation data
along the axial distance of
ball screw at $t = 3{,}600$ s

The comparisons of predictions with the experimental data indicated that the
FEM method could reasonably predict the thermal expansion process for deter-
mining the deformation of a ball screw system. Thus, calculations were extended
to consider the influences of different spindle speeds and traveling distance of the
nut on the temperature rises and thermal deformations of a ball screw shaft.
Table 2 illustrates the numerical test details in terms of the rotating speed and

Table 2 Numerical test details in terms of the rotating speed and moving extent of the ball screw under the composite operating conditions

Time (s)	Speed (rpm)	Distance (mm)
300	2,000	900
300	2,000	500
300	3,000	900
300	1,000	500

moving extent of the ball screw under the composite operating conditions. In simulations, the shaft starts the operation at a speed of 2,000 rpm with a 900-mm moving distance of the nut for 300 s and next with a moving distance of 500 mm for 300 s, then changes to the speed of 3,000 rpm with a 900-mm moving distance for 300 s, and decreases the speed to 1,000 rpm with a 500-mm moving distance in the last 300 s. The axial spans, defined as the moving distance of the nut, are 900 and 500 mm from the center to the left and right ends of the ball screw, whereas the operating time and ambient temperature are 1,200 s and 27.7 °C, respectively.

In this analysis, the FEM method and experimental measurements were conducted simultaneously to predict the temperature increase and thermal deformation distributions for composite working states. Three monitoring points (corresponding to #1, #2 and #3) were selected at the axial distance of 0.045, 0.871 and 1.45 m to probe the temperature variations. Figure 10 shows a comparison of the predictions with the measured temperature data along the axial distance of ball screw at $t = 1,200$ s. The results revealed that the predicted temperatures relatively higher than those of the experimental values with the greatest discrepancy of around 1 °C under the composite operating conditions. Steep temperature gradients were viewed at two areas (with the axial distances of 0.3–0.5 and 0.8–1.2 m, respectively) of the screw shaft because of the frictional heat generation associated with the moving spans of the nut as well as the axial thermal conduction transfer to both ends of the shaft.

Under the composite operating conditions, Fig. 11 illustrates a comparison of the time histories of the predictions with the measured temperature of the ball screw at 1,200 s. At the pre-specified axial distances of 0.045, 0.871 and 1.45 m, all three temperature profiles increased in the first 600 s with the point #2 showing the steepest rate owing to a reduction of moving span from 900 to 500 mm during the period of 300 to 600 s. In response to an increase of the speed from 2,000 to 3,000 rpm with a 500-mm moving distance for 300 s, the higher heat production causes relatively faster temperature increases at both ends of the shaft during the period of 600 to 900 s. When the speed shifts to 1,000 rpm in the last 300 s, a lower heat source in a shorter central area (with a reduction of traveling span from 900 to 500 mm) can result in temperature drops at the points #1, 3 and a flatter temperature rise at the point #2 toward their measured values of 28.8, 41.2 and 32.5 °C, respectively, at $t = 1,200$ s. Overall, the FEM method reasonably predicted the temperature profiles with the maximum difference under 4.64 %.

Figure 12 shows a comparison of the prediction with measured positioning accuracy data from a laser interferometer along the axial distance of the ball screw

Fig. 10 Comparison of
prediction with measured
temperature data along the
axial distance of ball screw at
$t = 1,200$ s (under the
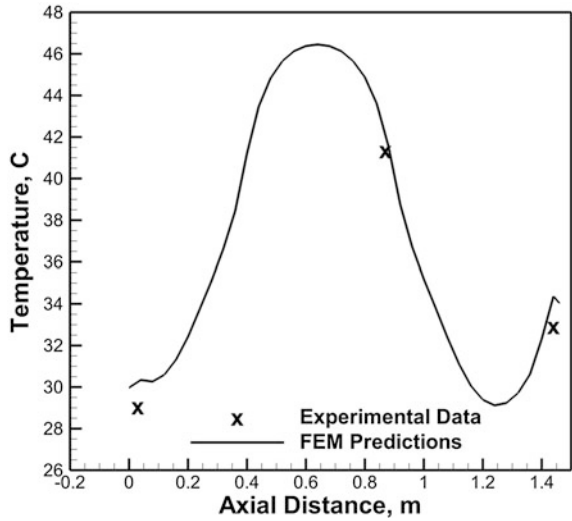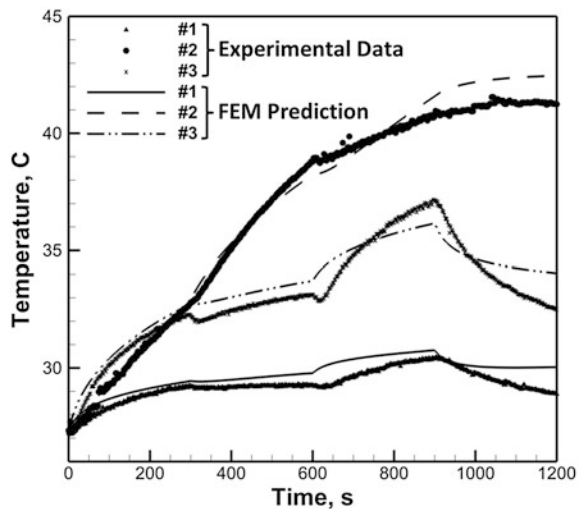composite operating
conditions)

Fig. 11 Comparison of the
time history of the predictions
with measured temperature
variation comparison at
1,200 s (under the composite
operating conditions)

at $t = 1,200$ s. The FEM predictions were in reasonable agreement with the experimental results, and the highest discrepancy was 6.5 % at the axial distance of 0.8 m. Essentially, the FEM method slightly under-predicted the thermal deformation, as compared to the measurements. In addition, it can be obviously observed that the thermal deformations increase with the axial distance from both the FEM predictions and measured results, leading to the deterioration of the positioning accuracy up to 152 μm. The simulated results suggested that the significant decline of the positioning accuracy as a result of vast heat production at high rotating speeds of shaft must be thermally compensated for a ball screw system in operation.

Fig. 12 Comparison of the
prediction with measured
positioning accuracy data
along the axial distance of the
ball screw at $t = 1,200$ s
(under the composite
operating conditions)
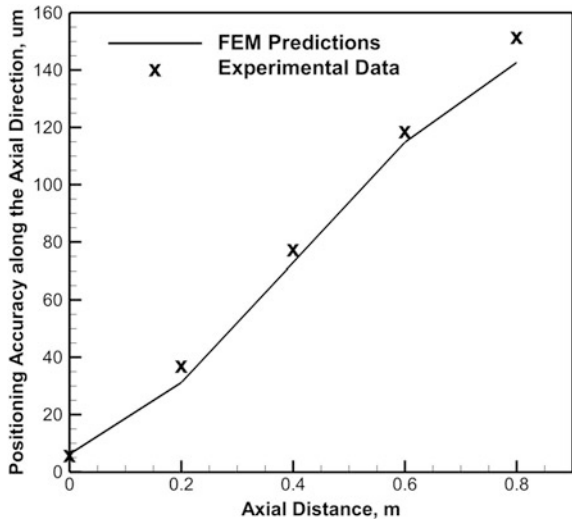
6 Conclusions

The position accuracy of a feed drive system was primarily influenced by the
thermal deformation of a ball screw. A high-speed ball screw system can generate
vast heat after long-term operations, with greater thermal expansion formed, and
thereby negatively impact the positioning accuracy of the feed drive mechanism. In
this research, the computational approach was applied using the FEM to simulate
the thermal expansion development for solving the deformation of a ball screw. In
simulations, we implemented the multi-zone heat loads to treat the heat generation
sources from the frictions between the nut, bearings and the ball screw shaft to
emulate reciprocating movements of the nut at a top speed of 40 m/min relative to
the shaft in a time period of 3.43 s. We also employed a three-dimensional unsteady
heat conduction equation to determine the steady and time-dependent temperature
distributions, as well as the temperature increases for calculating the thermal
deformations of the screw shaft. Simulations were extended to consider the com-
posite operating conditions involving various spindle speeds and moving spans of
the nut on the temperature rises and thermal deformations of a ball screw shaft.
Both the FEM-based simulations and measurements found that the thermal
deformations increased with the axial distance. The associated deformations can be
up to 152 μm at 0.8 m in composite operating situations, and in turn depreciated the
positioning accuracy. The computational and experimental results also indicated
that the significant deterioration of the positioning accuracy due to massive heat
production at high speeds of a shaft must be thermally compensated for a ball screw
system in operations.

References

1. R. Ramesh, M.A. Mannan, A.N. Po, Error compensation in machine tools—a review. Part II: thermal error. Int. J. Mach. Tools Manuf. **40**, 1257–1284 (2000)
2. W.S. Yun, S.K. Kim, D.W. Cho, Thermal error analysis for a CNC lathe feed drive system. Int. J. Mach. Tools Manuf. **39**, 1087–1101 (1999)
3. J. Bryan, International status of thermal error research. Ann. CIRP. **39**(2), 645–656 (1990)
4. R. Ramesh, M.A. Mannan, A.N. Po, Thermal error measurement and modeling in machine tools. Part I. Influence of varying operation conditions. Int. J. Mach. Tools Manuf. **43**, 391–404 (2003)
5. J.S. Chen, A study of thermally induced machine tool errors in real cutting conditions. Int. J. Mach. Tools Manuf. **36**, 1401–1411 (1996)
6. S. Li, Y. Zhang, G. Zhang, A study of pre-compensation for thermal errors of NC machine tools. Int. J. Mach. Tools Manuf. **37**, 1715–1719 (1997)
7. C.H. Lo, J. Yuan, J. Ni, An application of real-time error compensation on a turning center. Int. J. Mach. Tools Manuf. **35**, 1669–1682 (1995)
8. M. Xu, S.Y. Jiang, Y. Cai, An improved thermal model for machine tool bearings. Int. J. Mach. Tools Manuf. **47**, 53–62 (2007)
9. S. Koda, T. Murata, K. Ueda, T. Sugita, Automatic compensation of thermal expansion of ball screw in machining centers. Trans. Jpn. Soc. Mech. Eng. Part C. **21**, 154–159 (1990)
10. ANSYS, 13 User Guide. ANSYS Inc. Canonsburg, PA, USA (2010)
11. A.S. Yang, S.Z. Cai, S.H. Hsieh, T.C. Kuo, C.C. Wang, W.T. Wu, W.H. Hsieh, Y.C. Hwang, in *Thermal deformation estimation for a hollow ball screw feed drive system*. Lecture Notes in Engineering and Computer Science: Proceedings of The World Congress on Engineering, WCE 2013, 3–5 July, 2013, London, U.K., pp. 2047–2052
12. A. Verl, S. Frey, Correlation between feed velocity and preloading in ball screw drives. Ann. CIRP 59(2), 429–432 (2010)
13. T.A. Harris, *Rolling Bearing Analysis*. (Wiley & Sons, New York, 1991), pp. 540–560
14. H. Li, Y.C. Shin, Integrated dynamic thermo-mechanical modeling of high speed spindles, part I: model development. Trans. ASME, J. Manuf. Sci. Eng. **126**, 148–158 (2004)
15. Z.Z. Xu, X.J. Liu, H.K. Kim, J.H. Shin, S.K. Lyu, Thermal error forecast and performance evaluation for an air-cooling ball screw system. Int. J. Mach. Tools Manuf. **51**, 605–611 (2011)